MUTUAL INTERACTIONS OF FLOW STRUCTURE AND BUBBLE CAVITATION

Henda DJERIDI, Céline GABILLET, Jean-Yves BILLARD
IRENav, Institut de Recherche de l'Ecole Navale
BP 600, Lanvéoc Poulmic, 29240 Brest Naval FRANCE

Abstract

To quantify the interaction between the flow structures and the cavitating phase, the present experimental study focuses on the velocity measurements and spectral analysis by LDV of the liquid flow properties in a cavitating Couette Taylor flow. In this experiment, where the turbulent scales take place progressively, the bubbly phase is introduced in the gap by pressure drop and a particular attention is devoted to the determination of the effects of this bubbly phase on the properties of the flow by comparison between the single phase patterns and those observed in cavitating flow. This experimental work has highlighted the particular arrangement of the cavitating phase generated by the vortex pattern and the modification of the regimes existing in the single phase flow.

Nomenclature

R_i=30 mm	inner cylinder radius
R_o=35 mm	outer cylinder radius
Ω_i	rotating angular velocity
$d=R_o-R_i$ =5 mm	gap
$R_e = \frac{R_i \Omega_i d}{\nu}$	Reynolds number
Rec	critical Reynolds number
η=Ri/Ro=0.857	radius ratio
Γ=L/d =20	aspect ratio
d/Ri=0.16	clearance ratio
TVF:	Taylor Vortex flow Re_{c1}=102
WVF:	Wavy Vortex Flow Re_{c2}=138.4
MWVF:	Modulated wavy Vortex Flow Re_{c3}=1023
P_e	global pressure in the gap
P_v	vapor pressure
$\sigma = \frac{P_e - P_v}{\frac{1}{2}\rho (R_i \Omega_i)^2}$	cavitation index
$x = \frac{r}{d} - \frac{R_i + R_o}{2d}$	non dimensional radial position

1. Introduction

The majority of the studies conducted in two-phase flows were devoted to a better understanding of the fundamental mechanisms of mutual interactions between the dispersed phase and the liquid flow structure in many important engineering applications, such as the diffusion and transport process in centrifugal extractors or petroleum engineering systems. In hydrodynamic applications it is crucial to study cavitating turbulent flows because the structures of turbulent flows appear to be mainly responsible for the differences observed between the minimal pressure coefficient and the cavitation inception number. Concerning these mutual interactions, recent research testifies to the link between the turbulent structures and the cavitation inception. In 1986, the study by Katz and O'Hern on the turbulent wake of a sharp edged plate at high Reynolds number, clearly shows that the cavitation inception first occurred in the streamwise vortices mainly in the region situated between the transverse eddies but they did not quantify the observed interactions. O'Hern (1988) performed measurements of the pressure fluctuations in the shear layer using an air bubble injection method (Ooi and Acosta 1984), in the same kind of turbulent shear flow. He concluded that the experimental investigations of turbulent shear flows highlight the dominant role of the primary vortices in the overall flow field. He confirmed that the secondary structures control the cavitation inception because of the lowest flow pressures that occur in their cores.
Belahadji and Franc (1995) showed the existence of the same kind of coherent rotational structures in the far wake of a wedge. They also observed the presence of vortices that appear on the borders of the very near wake. They established that the cavitation is not a passive agent with respect to the basic flow, but that it reacts and

tends to modify the flow global features. The cavitation phenomenon breaks the connection between the elongation rate of vortex filaments and their rotation rate. The recent works of Keller (1997) and Keller and Rott (1997) relative to an experimental investigation of the effect of the turbulence intensity of the free stream flow on the cavitation behavior of submerged bodies, give more contribution. Regarding their overall results, they managed to dissociate the scale effects such as size, velocity, viscosity and the effects of flow turbulence on the cavitation phenomenon. They concluded that the observed discrepancies are due to the scale effects related to turbulent pressure fluctuations in the attached boundary layer of streamlined bodies, and that this turbulence causes an intense mixture of vortex tubes.

This non-exhaustive overview of research concerning cavitating turbulent flows has shown that there is a need of a detailed analysis of the interaction between the vapor phase and the flow structure in order to offer some answers to the following questions:
How can turbulent flow structures affect cavitation inception?
How can the presence of the vapor phase contribute to modify the state or feature of the liquid flow and, more generally speaking, are there any local or global characteristics of the vapor phase influencing the advance or the delay of the turbulent transition regime ?

To help answer these questions, we have chosen an academic Couette Taylor experiment. In this geometry the transition from laminar to turbulent flow occurs through a sequence of well defined instabilities. The goal is to study their possible interaction with the vapor phase as they successively occur in the flow, increasing progressively the turbulent spectrum. To achieve this, LDV measurements and visualization of the flow dynamic properties are made with and without vapor phase.

2. Experimental set-up

The experiments have been conducted in a vertical circular Couette apparatus, having an inner cylinder R_i, rotating at variable angular velocities, Ω_i. The flow is parameterized by the Reynolds number, the ratio of cylinder radii, the clearance ratio and the aspect ratio relative to the ratio of the fluid height to the gap between the cylinders. The Reynolds number Re can be varied by changing either the viscosity of the fluid or the rotation velocity of the inner cylinder. The apparatus is enclosed in an airtight chamber having, for visualization purposes, three transparent walls. The scheme of the Taylor Couette apparatus is given in Figure 1. The average reference pressure P_e of the chamber, is modified by using a vacuum pump and measured with a Kistler AW 1000 A10 sensor, ranging from 0 to 10^5 Pa, with a manufacture's accuracy of 200 Pa. LDV measurements using a two components, three beams, Dantec system and Burst Spectrum Analyzers (BSA) have been performed with an ellipsoidal measuring volume of 40µmx40µmx500µm, the largest dimension being in the radial direction, corresponding approximately to one-tenth of the gap. The time histories are registered with a data rate of 100 000 points per 30 seconds, which corresponds to a sample frequency of 3 kHz. This is a sufficiently high data rate compared to the characteristic frequency of the flow. The velocity mean and fluctuating parts, as well as the velocity time-histories have been measured according to a refined grid in the gap, in order to obtain the mean and turbulent flow properties and the motion topology.

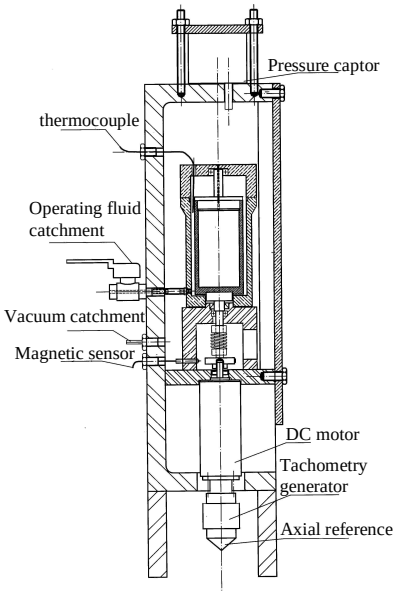

Figure 1 : General Schematics of the Taylor Couette apparatus with airtight chamber

3. Investigation of the mutual interactions

Bubbly phase arrangement

When the pressure is progressively decreased, for a fixed rotational velocity corresponding to the TVF regime (R_e/R_{ec1}=1), only up-travelling bubbles appear, governed by the buoyancy force, and no developed cavitating regime can be reached. On the other hand, for the WVF regime (R_e/R_{ec1}=3) and for a sufficient rotational velocity, the pressure drop leads to the apparition and capture of isolated bubbles, aligned along the azimuthal waves, in the kernel of the vortex structures. This arrangement is considered as the criterion of cavitation inception. The captured bubbles are arranged along each of the apparent azimuthal waves as a string of individual bubbles (Figure 2a to 2b), instead of a filled vapor tube as it can be observed in other kinds of vortices.

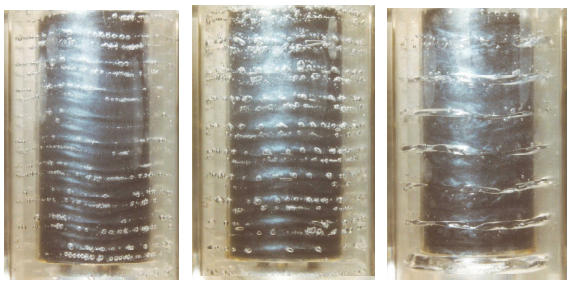

a) R_e/R_{ec1}=3.66 b) R_e/R_{ec1}=4.84 c) R_e/R_{ec1}=10.56

Figure 2: Photography of the cavitating flow, Pe~2700 Pa

The undulating bubble rings are arranged along the axis with alternating distances d_1 and d_2 respectively, equal to 1.2 and 0.8 times the gap for Re/Re_{c1} = 3.5. Those distances change progressively as the Reynolds number increases, d_1 becoming larger and d_2 smaller, until the fusion of the bubble rings in the outflow region. At this final state, the number of bubble rings in the gap is reduced by two, with an axial separate distance of about twice the gap. The bubbles have an elongated shape along the azimuthal waves (Figure 2c). The distorted inclusions seems also to be more dispersed around the Taylor center, constituting larger rings located near the inner cylinder.

Beyond Re/Re_{c1}=40, the formation of bubble rings, corresponding to the onset of the cavitating regime, can be observed above a pressure of P_e=2000 Pa in the airtight chamber. It is noticeable that the pressure P_e of cavitation inception increases with the Reynolds number, because of the associated annular flow participating directly to the local pressure drop. The distance between each bubble rings equals approximately the axial length of the Taylor Couette flow at the onset of cavitation, the dispersed phase remaining near the inner rotating cylinder, at every alternate boundary. This particular organization has already been observed by Atkhen *et al*. (1999) in highly turbulent ventilated Couette Taylor flow, where the dispersed phase (air bubbles) was considered as a passive tracer of the flow structures. In fact, when the pressure drop of the airtight chamber is performed at a fixed Reynolds number, the distance between two bubble rings increases progressively with cavitation development (Figure 3). The lower ring remains at the bottom of the apparatus, while the upper rings are progressively driven up from bottom to top. The number of cavitating rings N, stacked on the entire height of the gap decreases from 10 to 5 during the pressure drop. During this particular regime, the bubble rings remain located near the inner rotating cylinder in the outflow streamlines. The variation of the distance between two rings correspond in fact to a modification of the axial wavelength, with the developed cavitation acting this time, as an active tracer.

When the number of rings is reduced to 5, the situation either stabilizes or gives rise to a new regime. In this case, the lower bubble ring begins to climb up having been fixed until then to the bottom. The distance between rings remain approximately constant, all the cavitating structures being driven by the same axial motion from bottom to top. When the upper ring leaves the gap, a new one appears at the bottom and so on. The number of rings alternates successively between 5 and 4 until the complete degassing of the fluid.

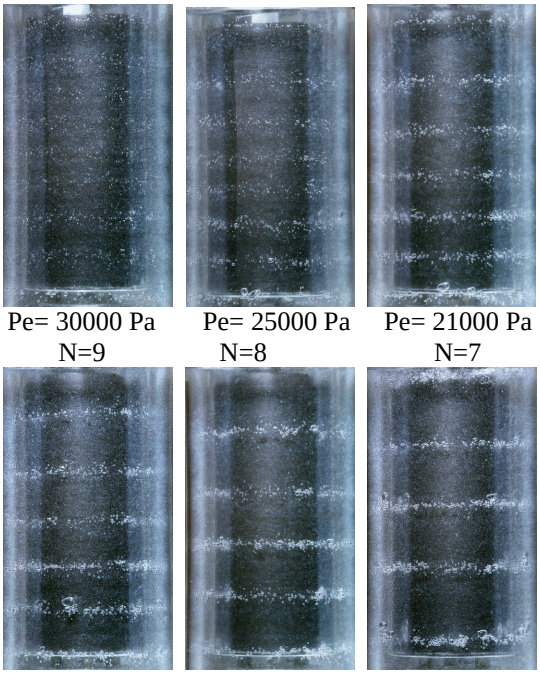

Figure 3: Behavior of the bubble rings with the pressure at Re/Re_{c1}=180

Cavitating effects of the flow structure

In order to study the cavitating effects of the flow structure, the axial and azimuthal velocity components have been recorded with a measurement grid of 651 points with a 0.25 mm spacing in the radial direction and 0.5 mm in the axial direction (corresponding respectively to 0.05d and 0.1d). Figure 4 presents the evolution of the axial velocity iso-contours in (x,z) plane with the dimensionless radial position x, z being the axial position. These figures show an example where the positive and negative components illustrate the well known Taylor vortex structure. In order to give more insight into the Taylor cells, the contours presented here correspond to the velocity levels, normalized by ν/d, following a linear increment.

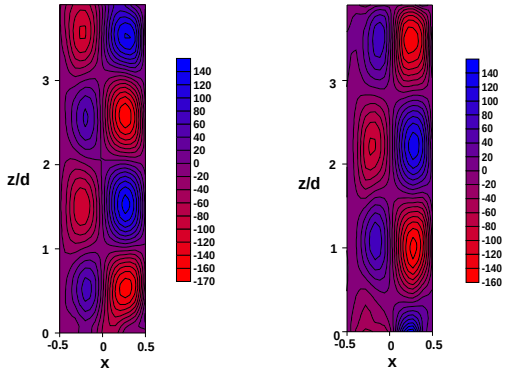

Figure 4: Comparison of the iso-contours of the axial velocity component at Re/Re_{c1}=10,
a) Single phase flow, b) Cavitating flow, P_e=2000 Pa.

At Re/Re_{c1}=10 in the single phase flow, the axial wavelength λ is defined as 2L/nd (where L is the height of the fluid column and n is the number of axial vortices). The comparison of the cartographic velocity representation of single phase flow figure 4a and cavitating flow figure 4b (with a vacuum chamber pressure P_e= 2000 Pa) show clearly, that the axial wavelength is increased by 25 % and the value is 2.5d rather than 2d in the single phase flow at WVF regime.

To quantify the impact of the cavitating phase, a spectral analysis has been performed on time series of axial velocity in the gap for Re/Re_{c1}=7.5, for the WVF regime with and without cavitation. The different spectrum are presented on Figure 5a and 5b.

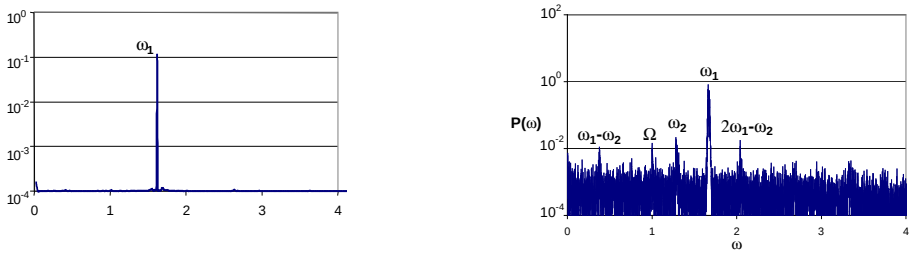

a) b)

Figure 5: Comparison of spectra obtained at Re/Re_{c1}=7.5, a) Single phase flow, b) Cavitating flow, P_e=2000 Pa.

In the single phase situation (Figure 5a) the estimated spectrum contains one normalized fundamental frequency ω_1 characterizing the second instability, ω=1 corresponding to the cylinder frequency Ω_i. At this Reynolds number, the non dimensional frequency equals 1.66 as observed with the stroboscopic light. The observed azimuthal wave number m_1 is 5 and the phase velocity ω_1/m_1 is about 0,33.

In the cavitating regime, the spectrum (Figure 5b) presents two fundamental frequencies ω_1 and ω_2, and their integer linear combination. The azimuthal wave number m_1 is identical and ω_1 still equal 1.66 with consequently the same phase velocity. The second fundamental frequency ω_2 emerges at 1.3. Repeated experiments realized, with and without cavitation in the annular gap, show that the modification of the wave number occurs earlier in the presence of the vapor phase. Figure 6 gives an example of the evolution of the azimuthal frequency versus Re/Re_{c1}.

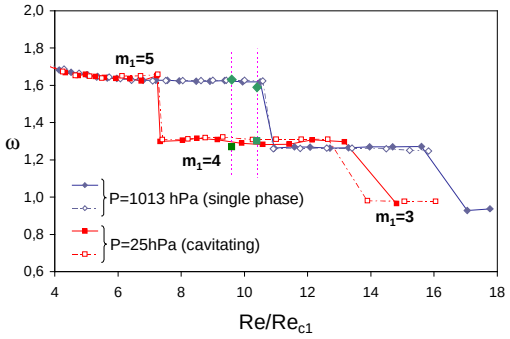

Figure 6: Evolution of the azimuthal frequency and the wave number versus reduced Reynolds number, with and without cavitation

At ambient pressure, without the vapor phase, the step change of the azimuthal frequency (5/4 and 4/3) occurs respectively at Re/Re_{c1}=10.5 and 16. With the dispersed phase, those latter frequencies appear at Re/Re_{c1}=7.2 and 13. Each evolution corresponds to a modification of the associated wave number, so leading for the same reduced Reynolds number to different states of flow according to whether the flow is cavitating or not. In this case, the Taylor history is unchanged and the multiplicity of the state flow observed by Coles (1965) can not be advanced, thus the observed modifications undoubtedly result from cavitation inception. The advance to the third instability, the premature change of the azimuthal wave number and the increase of the axial wave number in the cavitating flow regime seems to point out an earlier transition to turbulence.

For larger Reynolds numbers (corresponding to the weak turbulent regime), these interactions can be clearly seen through an axial evolution of the axial velocity component at the radial position $x = -0.25$. Indeed, for the single phase flow, despite the relatively large Reynolds number value, the passage from the positive to the negative velocity value corresponds to the distance between the cells, and that the value increases with the Reynolds number until 3.2d. When the cavitation is developed for example at Re/Re_{c1}=230 and P_e=15 000 Pa (Figure 7) , the distance variation between the two rings corresponds, in fact, to a modification of the axial wavelength and that this distance increases noticeably until 4.2. This behavior testifies that the vapor phase is an active tracer of the flow.

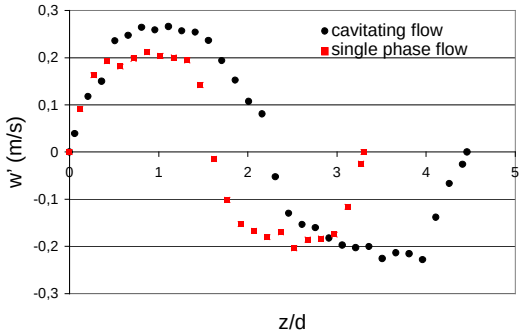

Figure 7: Axial evolution of axial velocity component for the radial position x=-0.25, at Re/Re_{c1} = 230, in single phase flow and cavitating flow, P_e=15000 Pa.

At the inception of the cavitation, for the sufficiently high pressure and at the beginning of the bubble rings arrangement, the vapor phase remains a passive tracer. In this case, the structure of the flow is not modified. However, the increase of the axial wave length and the advance to the third instability testify that the vapor phase can be considered as an active tracer and modify the topology of the flow. This behavior is observed for the low pressure when Re/Re_{c1} is greater than 7.5.

4. Cavitation index measurements

The evolution of the cavitation number is reported in Figure 8a and 8b for reduced Reynolds numbers ranging between 3 and 400. In the weak turbulence regime ($Re/Re_{c1}>40$), the cavitation number decreases as the Reynolds number increases. Notice that the data are quite scattered for a reduced Reynolds number ranging between 3 and 40, values corresponding to the first instabilities and the transition to turbulent regime. On Figure 8 b, the same data have been plotted in a logarithmic representation. It is clear that $Log(\sigma)$ evolves linearly as a function of $Log(Re/Re_{c1})$. This trend is observed for the range of reduced Reynolds numbers corresponding to the WVF regime, where $\sigma = C_1 (Re/Re_{c1})^{-2}$, and as well, for the turbulent regime where σ obeys the following relation: $\sigma = C_2 (Re/Re_{c1})^{-\frac{3}{2}}$. For Re/Re_{c1} less than 10, this behavior can be easily explained as $Re \sim \Omega_i$, $\sigma \sim \Omega_i^{-2}$. In this domain the value of P_e remains constant indicating that cavitation inception occurs for a constant pressure value in the gap corresponding to the critical pressure of the nuclei. For Re/Re_{c1} greater than 40, the modification of the exponent must be related to a modification of Pe at cavitation inception. It must be that this effect is introduced by local dynamic effects on nuclei due to the turbulent evolution of the flow state. Concerning the transition zone, corresponding to $10<Re/Re_{c1}<40$, a scattered behavior of cavitation index is observed. Notice that this range of reduced Reynolds numbers corresponds to the MWVF regime, the transition to turbulence and finally to the formation of the vapor filament localized near the inner cylinder. For this Reynolds number range, the aspect of the Taylor cells becomes more irregular and the flow inside the cells becomes more turbulent. The interplay between the large and small scales appears and attests to the transition to turbulence. Indeed, some authors Biage *et al.* (1996), Wei *et al.* (1992), explained this interplay by the generation of Görtler vortices which develop inside the Taylor cells close to the wall of the inner cylinder in the outflow region. In spite of the limited set of data obtained in the transition to turbulence regime, the scattered conditions observed in this area are assumed to be the consequence of an earlier breakdown of Taylor cells to smaller scale turbulence due to the dispersed phase.

The linear evolution of $Log(\sigma)$ as a function of Log(Re) has often been reported in works by numerous authors examining turbulent flows. For instance, Belahadji and Franc (1995) found the existence of $\sigma \sim Re^{1/2}$ relationship in the wake of a wedge. Fruman *et al.* (1993) investigated the prediction problem of cavitation inception in the tip vortex appearing on the elliptic planform hydrofoil, obtaining a linear evolution of the cavitation index for low Reynolds numbers and large Reynolds numbers corresponding to a turbulent regime. For the transition regime, they observed an intense scattering of the cavitation index. On the contrary, Arndt and Keller (1992), on the study of the effects of water quality on the cavitation inception in a turbulent wake, found that the cavitation index in the wake decreased with the velocity. In any case, even if work need to be devoted to the understanding of cavitation inception in transitional flows where the small scales appear progressively, the relationship between σ and Re is a power law in both laminar and turbulent flows.

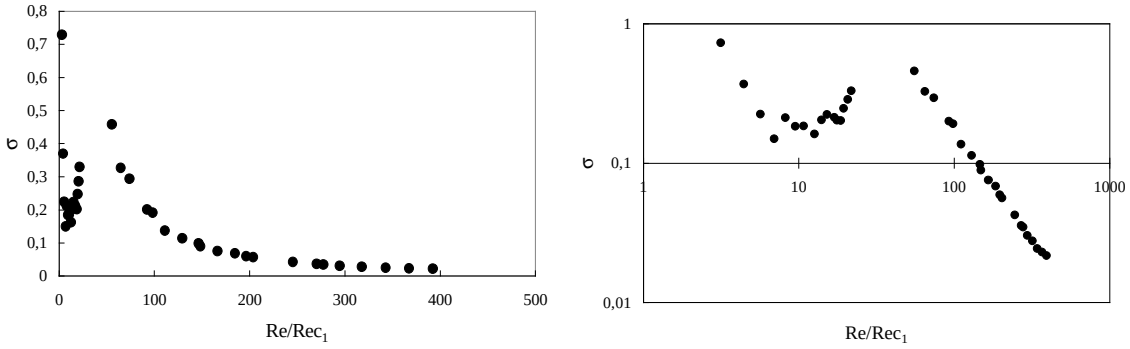

a) b)

Figure 8: a) Cavitation number versus reduced Reynolds number, b) logarithmic representation.

5. Conclusions

Two main results are obtained from the velocity measurement and visualizations. For the primary instabilities, the vapor phase gives rise to significant modification of the state flow: the axial wavelength is increased (25%) for the same Reynolds number and the continuous variation of the azimuthal wave frequency appears earlier (Re/Re_{c1}=7.2 instead of the usual critical value of 10.5). In weak turbulence, the vapor phase interacts with the flow and modifies the axial wavelength of the Taylor cells still present (at Re/Re_{c1}=230, λ/d=4.2 in cavitating flow instead of 3.2 in single phase flow), leading to establishing a new regime with a particular "leakage"-like dynamic. Thus, the earlier breakdown of Taylor cells to smaller scale turbulence is due to the bubble's dynamic behavior and to the vacuum rate of the dispersed phase. Work is in progress to investigate quantitatively these different effects.

Acknowledgements

The Authors are grateful for support from the French Navy.

References

J. Katz, T.J. O'Hern (1986). Cavitation in large scale shear flows. *Journal of Fluids Engineering, Transactions of the ASME* **108**: 373-376.

T.J. O'Hern (1988). cavitation inception in a turbulent shear flow. *American Institute of Aeronautics and Astronautics*, Cincinnati, 1621-1628.

K.K. Ooi, A.J. Acosta (1984). The utilization of specially Tailored air bubbles as static pressure sensors in a jet. *Journal of Fluid Engineering, Transactions of ASME* **106**: 459-465.

B. Belahadji, J.P. Franc (1995). Cavitation in the rotational structures of a turbulent wake. *Journal of Fluids Mechanics*, **287**: 383-403.

A.P. Keller (1997). The effect of flow turbulence on cavitation inception. *ASME Fluids Engineering Division Summer Meeting, Vancouver*.

A.P. Keller , H.K (1997). Rott. The effect of flow turbulence on cavitation inception. *ASME Fluids Engineering Division Summer meeting, Vancouver*.

K. Atkhen, J. Fontaine, J.L. Aider, J-E. Wesfreid (1999). Bulles dans un écoulement de Couette-Taylor. *C.R. Acad. Sci. Paris, t.327, **Série II b***, 207-213.

H**.** Djéridi, J.F. Favé, J.Y. Billard, D.H. Fruman (1999). Bubble capture and migration in Couette-Taylor flow *", Experiments in Fluids* **26**: 233-23.

D. Coles. Transition in circular Couette flow (1965). *Journal of Fluid Mechanics*, **21**:385-425.

M. Biage, S.R. Harris, W.R. Lempert, A.J. Smits (1996). Visualization study of Taylor Couette flow: description of the transition to turbulence. *27th AIAA Fluid Dynamics Conference.* New Orleans.

T. Wei, E.M. Kline, S.H.K. Lee, S. Woodruff (1992). Görtler vortex formation at the inner cylinder in Taylor-Couette flow. *Journal of Fluid Mechanics*, **245**, pp.47-68.

D.H. Fruman, P. Cerruti, T. Pichon (1993). On tip vortex turbulence, wandering and cavitation occurrence. *Second International Symposium on Cavitation. Tokyo, Japan.*

R.E.A Arndt, A.P. Keller (1992). Water quality effects on cavitation inception in a trailing vortex. *Trans. ASME, Journal of Fluids Engineering*, **114**:430-438.